

Symanzik Improvement In The Static Quark Potential

Frédéric D. R. Bonnet^{1*}, Derek B. Leinweber^{1†}, Anthony G. Williams^{1,2‡},
James M. Zanotti^{1§}

¹*Special Research Center for the Subatomic Structure of Matter (CSSM) and
Department of Physics and Mathematical Physics, University of Adelaide 5005, Australia.*

²*Department of Physics and SCRI, Florida State University, Tallahassee, FL 32306-4052*

(April 12, 2018)

Abstract

A systematic investigation of Symanzik improvement in the gauge field action is performed for the static quark potential in quenched QCD. We consider Symanzik improved gauge field configurations on a $16^3 \times 32$ lattice with a relatively coarse lattice spacing of 0.165(2) fm. A matched set of Standard Wilson gauge configurations is prepared at $\beta = 5.74$ with the same physical volume and lattice spacing and is studied for comparison. We find that, despite the coarse lattice spacing, the unimproved and less-expensive Wilson action does as well as the Symanzik action in allowing us to extract the static quark potential at large $q\bar{q}$ separations. We have considered novel methods for stepping off-axis in the static quark potential which provides new insights into the extent to which the ground state potential dominates the Wilson loop correlation function.

PACS number(s): 12.38.Aw, 12.38.Gc, 12.39.Pn, 14.70.Dj

*E-mail: fbonnet@physics.adelaide.edu.au

†E-mail: dleinweb@physics.adelaide.edu.au

‡E-mail: awilliam@physics.adelaide.edu.au

§E-mail: jzanotti@physics.adelaide.edu.au

I. INTRODUCTION

While string breaking in the static quark potential of full dynamical-fermion QCD has long been predicted, direct observation of string breaking in lattice QCD is proving to be elusive [1–7]. The main reason for this appears to be due to difficulty in isolating the ground state of the static quark potential at large $q\bar{q}$ separations [7]. Overlap of standard operators for separating a static $q\bar{q}$ pair with excited states of the potential and close spacing in the spectrum of the potential at large separations demand significant Euclidean time evolution in order to isolate the ground state [7–9].

Accessing large Euclidean times is extremely difficult. APE smearing [10] is widely recognized as an effective way to approach this region. The smearing of the spatial links of the lattice mocks up the flux tube joining two static quarks in the ground state potential. The smeared operator provides better overlap between the vacuum and the ground state potential and improves the signal to noise ratio in the correlation function [11].

As one approaches the large Euclidean space-time regime, statistical errors grow exponentially. While it is easy to fit the lattice data for the effective potential to a plateau ansatz, it is difficult to have confidence that the asymptotic value has been reached. With exponentially growing error bars, correlated χ^2 and goodness of fit parameters can provide a lower bound on the Euclidean time regime, but do not provide information on whether such a bound is sufficient to isolate the ground state potential.

Techniques for evaluating the extent to which the ground state dominates the Wilson loop are needed. Fortunately for the standard Wilson gluon action, methods exist. However, these methods break down when improved actions are used.

Recently, novel ideas have been explored in the search for string breaking [7,12–14]. We are motivated by the encouraging results of Ref. [7] studying string breaking via Wilson loops in $2 + 1$ dimensional QCD. There, using improved actions on coarse lattices in three dimensions, string breaking was observed. These authors emphasize that Euclidean time evolution of the order of 1 fm is required to isolate the ground state potential. The efficiency afforded by the use of coarse lattices is argued to be key to achieving this goal.

Here we explore a systematic comparison of the static quark potential obtained from standard Wilson and Symanzik improved field configurations. Given the same number of configurations, similar lattice spacing and equivalent analysis techniques, we illustrate how the Standard Wilson action does as well as the Symanzik improved action in extracting the long-range $q\bar{q}$ potential. While the authors of Ref. [7] emphasize the efficiency of the improved action approach, we find that unimproved actions on reasonably coarse lattices offer the most efficient and suitably accurate use of limited computer resources.

Section II briefly explains our technique for calculating the static quark potential from Wilson loops. Here we present an alternative way of exploring the off-axis static quark potential. This new method provides additional information on the extent to which the ground-state potential dominates the Wilson loop and can provide confidence that sufficient evolution in Euclidean time has occurred. Section III outlines the Symanzik improved action. In Section IV, we present and discuss our results and conclude in Section V.

II. THE STATIC QUARK POTENTIAL

The spectrum of the static quark potential is determined from Wilson loops $W(r, t)$ of area $r \times t$,

$$W(r, t) = \sum_i C_i(r) \exp(-V_i(r) t). \quad (1)$$

In order to enhance $C_1(r)$, which measures the overlap of the loop with the ground state potential, the spatial links are APE smeared [10]. This smearing procedure replaces a spatial link $U_\mu(x)$, with a sum of the link and α times its spatial staples:

$$U_\mu(x) \rightarrow (1 - \alpha)U_\mu + \frac{\alpha}{4} \sum_{\substack{\nu=1 \\ \nu \neq \mu}}^3 \left[U_\nu(x)U_\mu(x + \nu a)U_\nu^\dagger(x + \mu a) \right. \\ \left. + U_\nu^\dagger(x - \nu a)U_\mu(x - \nu a)U_\nu(x - \nu a + \mu a) \right]. \quad (2)$$

This is applied to all spatial links on the lattice followed by projection back to SU(3), and repeated n times.

Tuning the smearing parameters is key to the success of the approach. They govern both the Euclidean time extent of the Wilson loop correlation function and the relative contributions of ground to excited state contributions. It is vital to have a quantitative technique for tuning these parameters in order to optimise future studies of string breaking. The measure must be the extent to which the ground state dominates the correlation function.

Efficient methods exist for the unimproved Wilson action for fine tuning the smearing parameters to provide optimal overlap with the ground state potential. For $t = 0$, $W(r, t = 0) = 1$ providing the constraint $\sum_i C_i(r) = 1$ for a given r . For unimproved actions, where the transfer matrix is positive definite, each $C_i(r) \geq 0$. This means $C_1(r)$ can be monitored at large r but small t as the number of smearing sweeps are varied, with the optimal amount of smearing occurring when $C_1(r) \approx 1$. The proximity of $C_1(r)$ to 1 for small t may be easily estimated from the ratio

$$W^{t+1}(r, t)/W^t(r, t + 1) \quad (3)$$

which equals $C_1(r)$ in the limit $C_1(r) \rightarrow 1$. This provides a quantitative measure of ground-state-dominance for unimproved Wilson actions. We note that it is sufficient [15] to fix the smearing fraction, α , and explore the parameter space via the number of smearing sweeps, n .

This procedure can be repeated for a number of alternate paths of links for a given separation r . By using variational techniques as described in Ref. [16], the combination of paths that gives the greatest overlap with the ground state can be found.

Actions improved in the time direction do not satisfy Osterwalder-Schrader [17] positivity [18]. This spoils the positive definite nature of the transfer matrix and the constraint $C_i(r) \geq 0$ is lost. Hence one needs either a new quantitative measure for evaluating ground-state-dominance, or to check the merits for using Symanzik improved gluon actions for the static quark potential at large r .

For exploratory purposes, we fixed $\alpha = 0.7$ and considered the values $n = 10, 20, 30$ and 40 . The best results on a $16^3 \times 32$ lattice with lattice spacing ≈ 0.17 fm, are obtained using $\alpha = 0.7$ and $n = 10$ for the unimproved Wilson gauge action. This corresponds to a transverse RMS radius for the smeared links of 0.31 fm, where the transverse RMS radius after n sweeps is defined by

$$\langle r^2 \rangle_n = \frac{\sum_x x^2 V_n^2(x)}{\sum_x V_n^2(x)} \quad (4)$$

where

$$V_i(x') = \sum_x \left[(1 - \alpha) \delta_{x'x} + \frac{\alpha}{4} \sum_{\mu=1}^2 (\delta_{x',x+\mu} + \delta_{x',x-\mu}) \right] V_{i-1}(x)$$

and

$$V_0(x) = \begin{cases} 1 & x = 0 \\ 0 & x \neq 0 \end{cases}.$$

Analogous to the RMS smearing radius of Jacobi Fermion Source Smearing [19], this provides a reasonable estimate of the transverse smearing of mean field improved links ($U_\mu(x) \sim 1$).

Wilson loops, $W(r, t)$, or more precisely $W(x, y, z, t)$ where $r^2 = x^2 + y^2 + z^2$, are calculated both on-axis, along the Cartesian directions, and off-axis. On-axis Wilson loops are those that lie, e.g., in the $x - t$ plane only; off-axis loops begin, for example, by first stepping into the y or z (or both) directions before proceeding through the $x - t$ plane.. This provides an alternative to the usual method of calculating the off axis potential by building paths in three different directions using small elemental squares, rectangles or cubes and multiplying them together to form larger paths (see, for example, Ref. [20]). These standard techniques for calculating the off-axis potential may be combined with the approach described here using the variational method described extensively in Ref. [16].

Due to the periodicity of the lattice, the size of our Wilson loops are limited from 1 to a little over half the smallest lattice dimension in the on-axis directions and between 0 and 3 in the transverse directions. For example, for a $16^3 \times 32$ lattice, the sizes of the Wilson Loops, $t \times x \times y \times z$, vary from a $1 \times 1 \times 0 \times 0$ loop, to a $10 \times 10 \times 3 \times 3$ loop. Statistics are improved by transposing the loops over all points on the lattice and by rotating through the three spatial directions

In order to efficiently calculate Wilson loops of various sizes, including off-axis loops, we build products of links in each direction that we are considering for our Wilson loop. Link products extending from every lattice site are calculated in parallel. The loops are then formed in parallel by multiplying the appropriate sides together. Each side is created by reusing the components of the previous loop and one additional link. The same approach can be extended to loops that travel off-axis.

In an attempt to isolate the ground state potential for off-axis paths, one symmetrizes over the path of links connecting the off-axis heavy quark propagators, exploiting the full cubic symmetry of the lattice. For example, two points separated by n_x sites in the x -direction, n_y sites in the y -direction and n_z sites in the z -direction, may be connected by n_x link products in the x -direction, n_y link products in the y -direction and n_z link products in the z -direction which we denote by the triplet xyz . Instead of only calculating off-axis paths in the specific order xyz , we average over spatial paths calculated in the order

$xyz, xzy, yxz, yzx, zxy, zyx$. We calculated loops using this path-symmetrized technique as well as loops using a non-path-symmetrized operator where the order xyz alone is considered. The former form of operator is designed to suppress excited states by incorporating the full hyper-cubic symmetry of the lattice, whereas the latter operator is susceptible to excited state contamination. By comparing the static quark potential for these two operators, one can gain qualitative information on the effect of excited states in the static quark potential.

III. NUMERICAL SIMULATIONS

The tree-level $\mathcal{O}(a^2)$ -Symanzik-improved action [21] is defined as,

$$S_G = \frac{5\beta}{3} \sum_{\text{sq}} \mathcal{R}e\text{Tr}(1 - U_{\text{sq}}(x)) - \frac{\beta}{12u_0^2} \sum_{\text{rect}} \mathcal{R}e\text{Tr}(1 - U_{\text{rect}}(x)), \quad (5)$$

where the operators $U_{\text{sq}}(x)$ and $U_{\text{rect}}(x)$ are defined as follows,

$$U_{\text{sq}}(x) = U_\mu(x)U_\nu(x + \hat{\mu})U_\mu^\dagger(x + \hat{\nu})U_\nu^\dagger(x) \quad (6)$$

$$U_{\text{rect}}(x) = U_\mu(x)U_\nu(x + \hat{\mu})U_\nu(x + \hat{\nu} + \hat{\mu})U_\mu^\dagger(x + 2\hat{\nu})U_\nu^\dagger(x + \hat{\nu})U_\nu^\dagger(x) \\ + U_\mu(x)U_\mu(x + \hat{\mu})U_\nu(x + 2\hat{\mu})U_\mu^\dagger(x + \hat{\mu} + \hat{\nu})U_\mu^\dagger(x + \hat{\nu})U_\nu^\dagger(x). \quad (7)$$

The link product $U_{\text{rect}}(x)$ denotes the rectangular 1×2 and 2×1 plaquettes. u_0 is the tadpole improvement factor that largely corrects for the quantum renormalisation of the operators. We employ the plaquette measure

$$u_0 = \left(\frac{1}{3} \mathcal{R}e\text{Tr}\langle U_{\text{sq}} \rangle \right)^{1/4}. \quad (8)$$

Eq.(5) reproduces the continuum action as $a \rightarrow 0$, provided that β takes the standard value of $6/g^2$. Perturbative corrections to this action are estimated to be of the order of two to three percent [22].

Gauge configurations are generated using the Cabibbo-Marinari [23] pseudoheat-bath algorithm with three diagonal $SU(2)$ subgroups. Simulations are performed using a parallel algorithm with appropriate link partitioning [24]. Configurations are generated on a $16^3 \times 32$ lattice at $\beta = 5.74$ using a standard Wilson action which corresponds to lattice a spacing $a = 0.165(2)$, and on a $16^3 \times 32$ lattice at $\beta = 4.38$ using the Symanzik improved action (Eq. 7) which also corresponds to a lattice spacing $a = 0.165(2)$ fm. Thus the two lattices have the same lattice spacing and physical volume.

Configurations are selected after 5000 thermalization sweeps from a cold start. The mean link, u_0 , is averaged every 10 sweeps and updated during thermalization. For both the standard Wilson action and the Symanzik improved action, configurations are selected every 500 sweeps. The following analysis is based on an ensemble of 100 configurations for each action.

IV. SIMULATION RESULTS

The effective potential is obtained from

$$V_t(r) = \log \left(\frac{W(r, t)}{W(r, t + 1)} \right), \quad (9)$$

which is expected to be independent of t for $t \gg 0$. Figure 1 displays the effective potential as a function of Euclidean time, t , obtained from 100 configurations generated via the Symanzik improved action at $\beta = 4.38$. For $r \geq 7$, we find that the signal is generally dominated by noise for $t > 4$, so we set the upper limit of our fitting range to $t_{\max} = 4$. The good plateau behavior at small Euclidean time is a reflection of the optimized smearing. Choosing the lower limit $t_{\min} = 1$ leads to large $\chi^2/\text{d.o.f}$ for large r . We fix the fitting range to be, in most cases, $t = 2$ to 4. The string tension is then extracted from the ansatz,

$$V(r) = V_0 + \sigma r - e/r \quad (10)$$

where $e = \pi/12$ [25], and V_0 and σ are fit parameters.

The values for $V(r) + e/r = \sigma r + V_0$ are then fitted to a line and the slope, σ , and intercept, V_0 , are extracted. We fit the range $3 < r < 7$ such that we are not sensitive to the coulomb term and its associated discretisation artifacts [26]. The error analysis is done using the Bootstrap method and all errors quoted are statistical only. Using $\sqrt{\sigma} = 440$ MeV to set the scale, the lattice spacings are determined.

A. Wilson Loop Correlation Function

To have any hope of seeing string breaking in QCD with dynamical fermions, the gauge links must first be smeared to improve the overlap of the ground state. The effects of smearing the spatial links (Eq. (2)) before calculating Wilson Loops is well known. Smearing provides access to the static quark potential at larger distances, providing a better chance of eventually being able to detect string breaking. Also, the lines with smeared links exhibit better plateau behavior in $V_t(r)$ than the unsmeared ones, indicating that we have better isolation of the ground state.

Figs. 1 and 2 illustrate the time dependence of Eq. 9 for Symanzik improved and standard Wilson gluon actions respectively. For clarity, we only plot values for r that are obtained from on-axis loops. For both the improved and unimproved actions, we see a clean signal up to $r \approx 8$ for the first three or four time slices. For r values greater than this, the quality of the statistical signal does not allow values of t larger than 2 or 3 to be included in the fits.

B. Off Axis Perturbations and Symmetry

Our method for stepping off-axis requires the use of a path-symmetrized operator. Fig. 3 displays results for the path-symmetrized operator for separating the $q\bar{q}$ pair, while Fig. 4 illustrates the non-path-symmetrized result. Both plots are obtained with 10 smearing

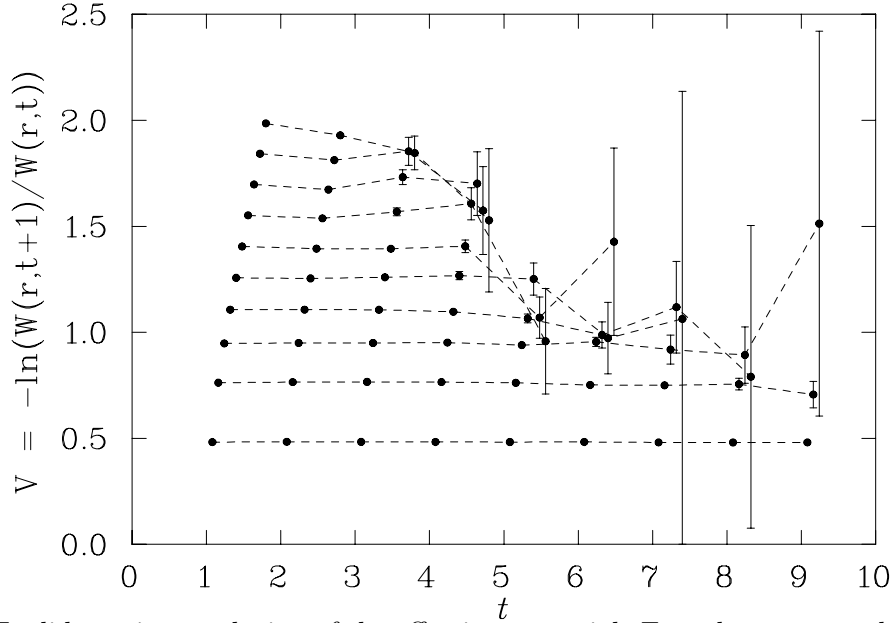


FIG. 1. Euclidean time evolution of the effective potential. From bottom up, the “horizontal” lines correspond to $r = 1$ through 10. Here we use the Symanzik improved action with $\beta = 4.38$ and 10 sweeps of smearing at $\alpha = 0.7$. Axes are in lattice units. Points are offset to the right for clarity.

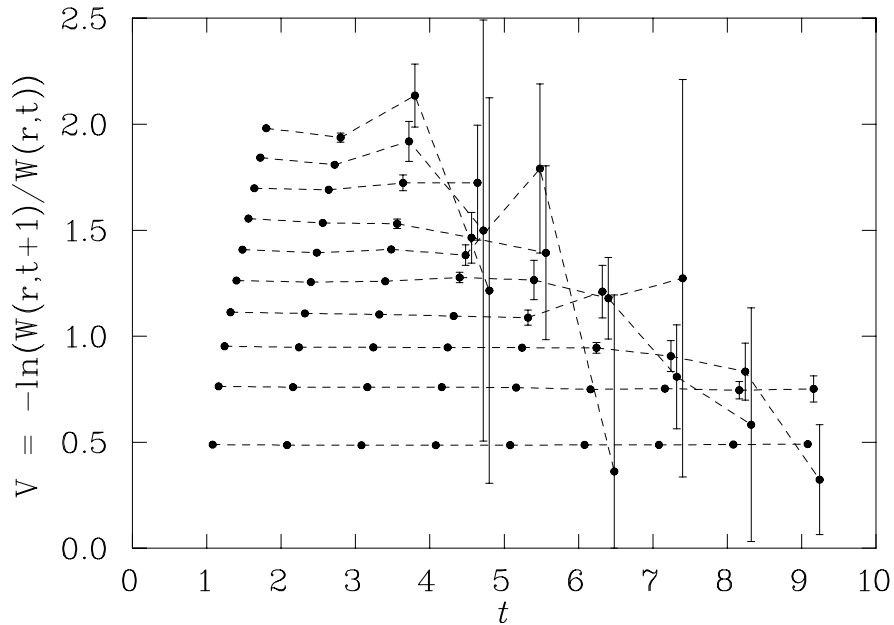


FIG. 2. Euclidean time evolution of the effective potential. From bottom up, the “horizontal” lines correspond to $r = 1$ through 10. Here we use the standard unimproved Wilson action with $\beta = 5.74$ and 10 sweeps of smearing at $\alpha = 0.7$. Axes are in lattice units. Points are offset to the right for clarity.

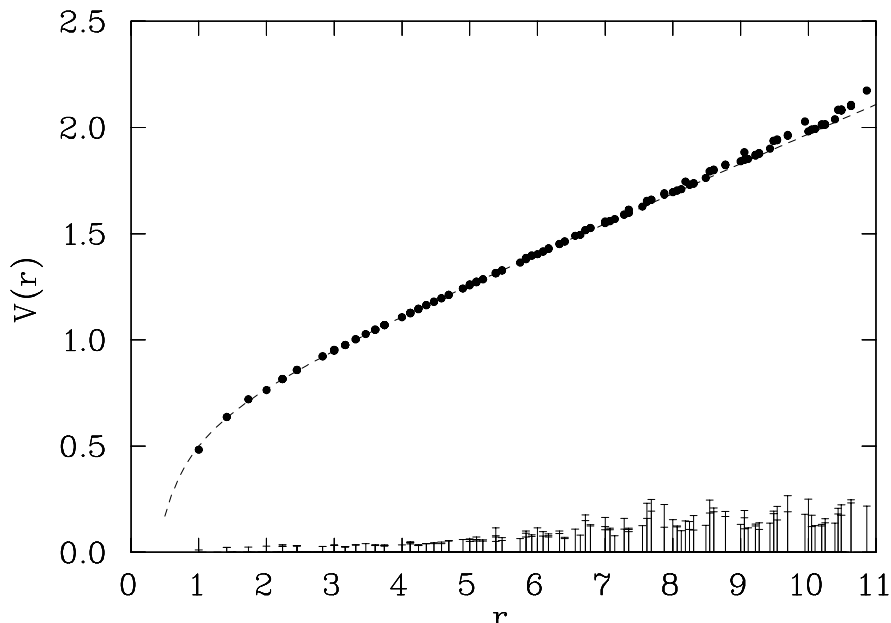


FIG. 3. The static quark potential, $V(r)$, as a function of the separation r . Data is from the Symanzik improved action at $\beta = 4.38$ with 10 sweeps of smearing at $\alpha = 0.7$ and a path-symmetrized operator. Time slices $t = 1$ to 4 are used in the fit of the correlation function. Error bars are magnified by a factor of 200 and placed on the r -axis for clarity.

sweeps at $\alpha = 0.7$. Banding is clearly evident in the non-path-symmetrized case but as soon as we path-symmetrize our operators, the banding largely disappears in off-axis points up to about $r = 7$. After $r = 7$, the banding still persists in off-axis points where loops of the form $r \times 1 \times 3$, $r \times 2 \times 3$ or $r \times 3 \times 3$ (where $r =$ on-axis step size and is greater than 7) are used. However the banding is negligible in off-axis points up to, and including, $r \times 2 \times 2$. Since our off-axis points are obtained by firstly stepping in one direction and then stepping in a different Cartesian direction, we are forming a right angle, not an approximate straight line. The fact that for $r < 7$, the $r \times 3 \times 3$ points lie on the line-of-best-fit is an interesting result and provides support for the use of this operator in a variational approach when searching for ground state dominance and its associated string breaking in full QCD. However, the persistence of banding at large r is an indicator that further Euclidean time evolution is required to isolate the ground state potential.

C. Effect Of Using Symanzik Improved Gauge Field Configurations

Historically, the main feature of improved gauge field actions is the improved rotational symmetry [22]. This can be seen in our configurations by comparing Figs. 5 and 6. These graphs are enlargements of the small- r area. The off axis points for the Symanzik improved $\beta = 4.38$ lattices lie closer to the line of best fit through the Cartesian points, $r = 3$ to 7, than the unimproved Wilson $\beta = 5.74$ lattices.

However, here we are most interested in the large distance properties of the Wilson loop.

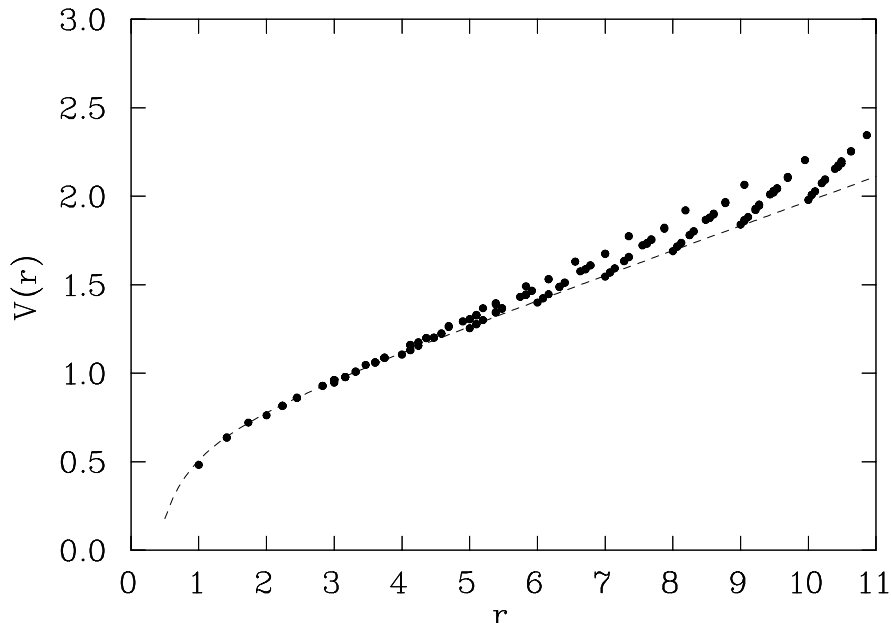


FIG. 4. The static quark potential, $V(r)$, as a function of the separation r . Data is from the Symanzik improved action at $\beta = 4.38$ with 10 sweeps of smearing at $\alpha = 0.7$ and a non-path-symmetrized operator. Time slices $t = 1$ to 4 are used in the fit of the correlation function. Statistical error bars are too small to be seen.

To draw firm conclusions on the merits of using Symanzik improved actions in the search for string breaking, we create a matched set of standard Wilson gluon configurations, tuned to reproduce the string tension of the $\beta = 4.38$ improved configurations.

Figs. 3 and 7 compare Symanzik improved and unimproved Wilson results for $V(r)$ extracted from correlated fits within the range $1 \leq t \leq 4$. A similar comparison is made with Figs. 8 and 9 within the range $2 \leq t \leq 4$. Magnified error bars are plotted on the X-axis to allow a comparison of signal to noise between the two actions. Exponential growth in the error bars for large r is apparent in the fits with $2 \leq t \leq 4$.

It is crucial to compare matched lattices with the same lattice spacing and same physical volume. For example, a comparison of an unimproved Wilson lattice with $\beta = 5.70$ and lattice spacing $a = 0.181(2)$, with a Symanzik improved lattice at $\beta = 4.38$ and $a = 0.165(2)$ leads one to incorrectly conclude that Symanzik improved actions lead to an improvement in the signal-to-noise ratio of the static quark potential at large $q\bar{q}$ separations. The unimproved configurations with $\beta = 5.70$ lose the signal around $r/a = 7.5$ ($r = 1.37$ fm) when using time slices $t = 2 - 4$, whereas the improved configurations hold the signal up to $r/a = 9.5$ ($r = 1.59$ fm) when using $t = 2 - 4$. This effect is due to the slightly larger lattice spacing in the $\beta = 5.70$ simulations, which spoils the signal-to-noise ratio even after the larger lattice spacing is taken into account.

Close inspection of Figs. 7 and 9, where the Euclidean time regimes $1 \leq t \leq 4$ and $2 \leq t \leq 4$ are compared, reveals how the off-axis points can also be used to gain confidence in ground state dominance. In Fig. 7, banding is apparent. However, upon adjusting the Euclidean time regime for the fit to larger times in Fig. 9, the banding is largely removed.

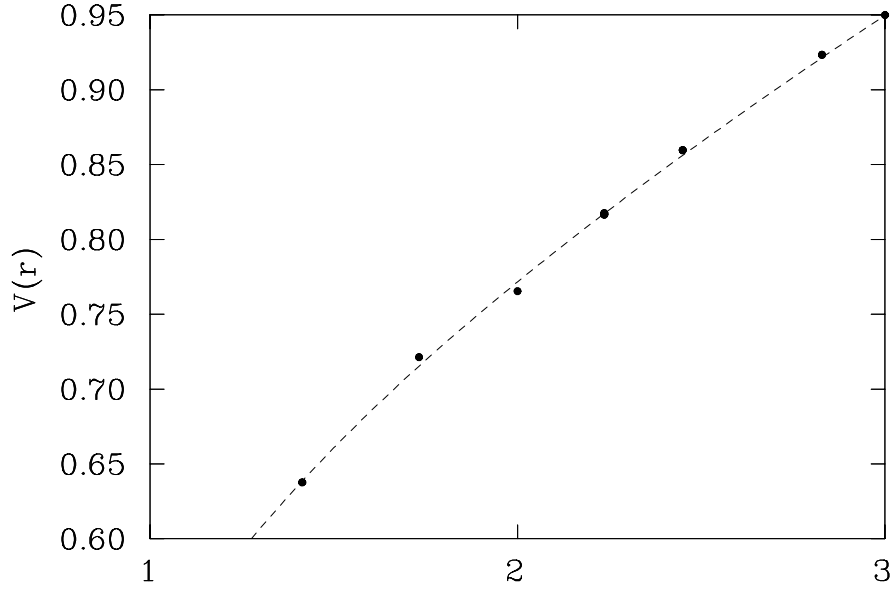


FIG. 5. A close up of the static quark potential, $V(r)$, as a function of the separation r . Data is from the Symanzik improved action at $\beta = 4.38$ with 10 sweeps of smearing at $\alpha = 0.7$ and a path-symmetrized operator. Time slices $t = 2$ to 4 are used in the fit of the correlation function. The dashed line is a fit of Eq. 10 to on axis points $r = 3$ to 7.

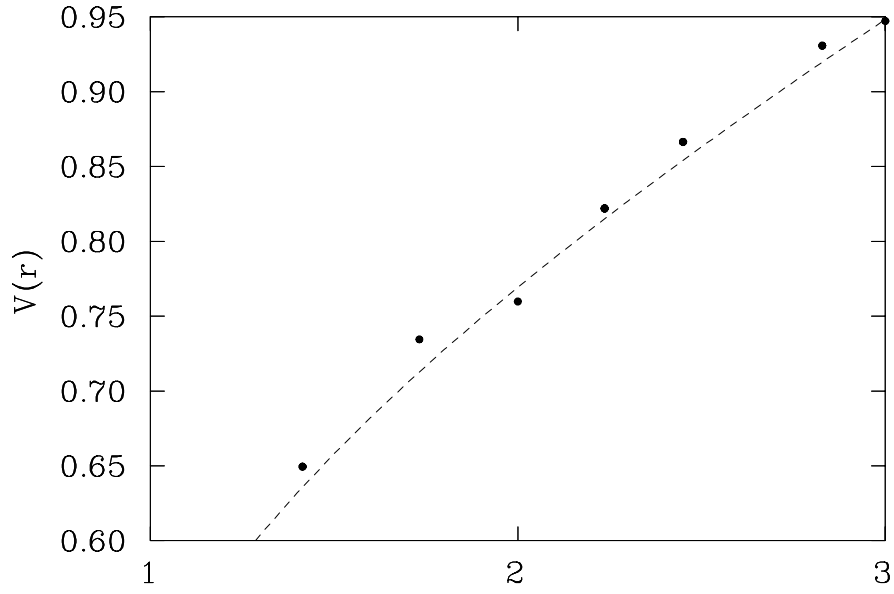


FIG. 6. A close up of the static quark potential, $V(r)$, as a function of the separation r . Data is from the unimproved Wilson action at $\beta = 5.74$ with 10 sweeps of smearing at $\alpha = 0.7$ and a path-symmetrized operator. Time slices $t = 2$ to 4 are used in the fit of the correlation function. The dashed line is a fit of Eq. 10 to on axis points $r = 3$ to 7.

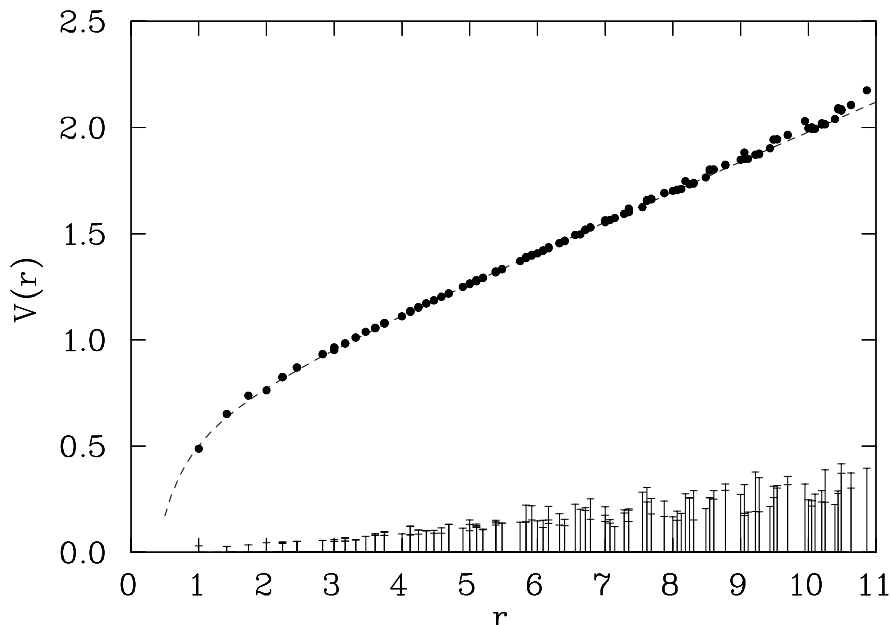


FIG. 7. The static quark potential, $V(r)$, as a function of the separation r . Data is from the unimproved Wilson action at $\beta = 5.74$ with 10 sweeps of smearing at $\alpha = 0.7$ and a path-symmetrized operator. Time slices $t = 1$ to 4 are used in the fit of the correlation function. Error bars are magnified by a factor of 200 and placed on the r -axis for clarity.

V. CONCLUSIONS

We have calculated the static quark potential in quenched QCD using Symanzik improved and unimproved Wilson gluon actions. We have kept the lattice spacing and the physical volume of these lattices equal so that we can meaningfully compare the results. The number of gauge field configurations (100 here) is also held fixed for each action. We have explicitly shown that, despite the relatively coarse lattice spacing, the unimproved and computationally less expensive Wilson action does just as well as the improved action in extracting the $q\bar{q}$ potential at large separations. If one wishes to keep non-perturbative physics such as non-trivial topological fluctuations on the lattice, then one needs $a < 0.15$ fm [27], and thus $r/a > 7$. In this case, the unimproved, standard Wilson gauge action is ideal for today's string breaking searches and computational resources can be redirected elsewhere. Another advantage for using unimproved Wilson gauge configurations is that we recover the extremely useful method for calculating the overlap with the ground state, $C_1(r)$, and thus tuning the smearing parameters.

We also explored the use of unconventional paths in accessing off-axis values of r in the static quark potential. These paths can provide insight into the extent to which the ground state potential dominates the Wilson loop at large Euclidean times. Provided the paths are symmetrized, these new paths provide useful information on the ground state potential and nearby excited potentials. Combined with standard paths and variational techniques, these paths offer additional promise for the search for string breaking in lattice QCD.

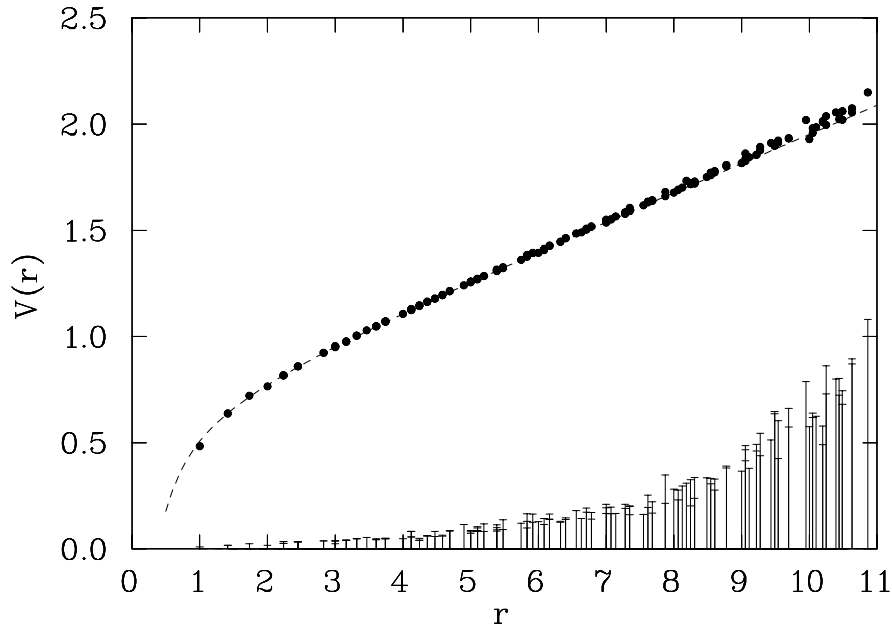


FIG. 8. The static quark potential, $V(r)$, as a function of the separation r . Data is from the Symanzik improved action at $\beta = 4.38$ with 10 sweeps of smearing at $\alpha = 0.7$ and a path-symmetrized operator. Here time slices $t = 2$ to 4 are used in the fit of the correlation function. Error bars are magnified by a factor of 200 and placed on the r -axis for clarity.

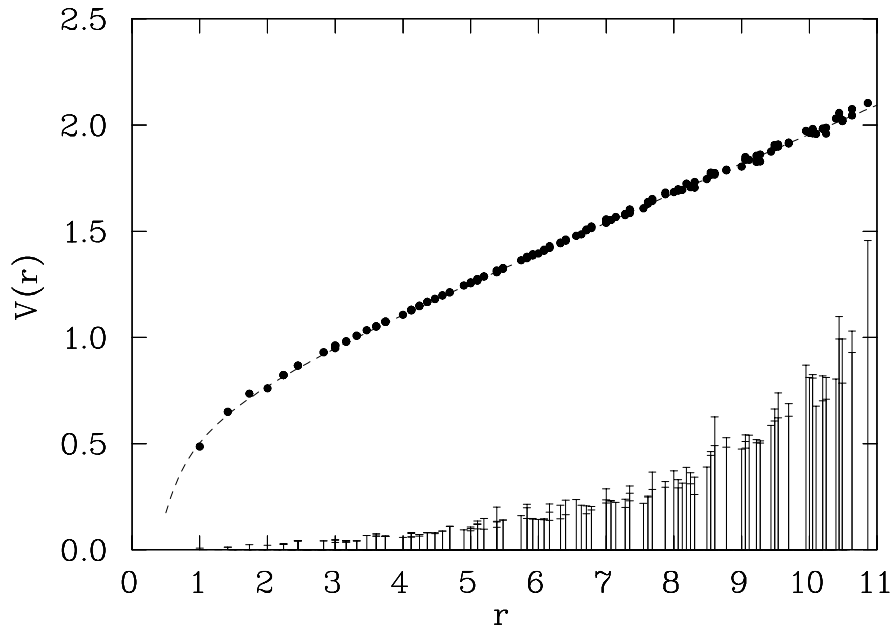


FIG. 9. The static quark potential, $V(r)$, as a function of the separation r . Data is from the unimproved Wilson action at $\beta = 5.74$ with 10 sweeps of smearing at $\alpha = 0.7$ and a path-symmetrized operator. Time slices $t = 2$ to 4 are used in the fit of the correlation function. Error bars are magnified by a factor of 200 and placed on the r -axis for clarity.

ACKNOWLEDGMENTS

This work was supported by the Australian Research Council and by grants of supercomputer time on the CM-5 made available through the South Australian Centre for Parallel Computing. We would also like to thank the National Computing Facility for Lattice Gauge Theory for the use of the Orion Supercomputer. AGW also acknowledges support from the Department of Energy Contract No. DE-FG05-86ER40273 and by the Florida State University Supercomputer Computations Research Institute which is partially funded by the Department of Energy through contract No. DE-FC05-85ER25000

REFERENCES

- [1] J. Kuti, Nucl. Phys. Proc. Suppl. **73**, 72 (1999) [hep-lat/9811021].
- [2] S. Aoki *et al.* [CP-PACS Collaboration], Nucl. Phys. Proc. Suppl. **73**, 216 (1999) [hep-lat/9809185].
- [3] M. Talevi [The UKQCD Collaboration], Nucl. Phys. Proc. Suppl. **73**, 219 (1999) [hep-lat/9809182].
- [4] G. S. Bali *et al.* [SESAM Collaboration], Nucl. Phys. Proc. Suppl. **63**, 209 (1998) [hep-lat/9710012].
- [5] A. Duncan, E. Eichten and H. Thacker, Phys. Rev. **D63**, 111501 (2001) [hep-lat/0011076].
- [6] P. Pennanen and C. Michael [UKQCD Collaboration], hep-lat/0001015.
- [7] H. D. Trottier, Phys. Rev. **D60**, 034506 (1999) [hep-lat/9812021].
- [8] S. Gusken, Nucl. Phys. Proc. Suppl. **63**, 16 (1998) [hep-lat/9710075].
- [9] I. T. Drummond, Phys. Lett. **B434**, 92 (1998) [hep-lat/9805012].
- [10] M. Falcioni, M. Paciello, G. Parisi, B. Taglienti, Nucl. Phys. **B251**, 624 (1985); M. Albanese *et al.*, Phys. Lett. **B192**, 163 (1987).
- [11] C. Legeland, B. Beinlich, M. Lutgemeier, A. Peikert and T. Scheideler, Nucl. Phys. Proc. Suppl. **63**, 260 (1998) [hep-lat/9709147].
- [12] C. DeTar, U. Heller and P. Lacock, Nucl. Phys. Proc. Suppl. **83**, 310 (2000) [hep-lat/9909078].
- [13] F. Knechtli, Nucl. Phys. Proc. Suppl. **83**, 673 (2000) [hep-lat/9909164].
- [14] F. Knechtli and R. Sommer [ALPHA Collaboration], Phys. Lett. **B440**, 345 (1998) [hep-lat/9807022].
- [15]
- [15] F. D. Bonnet, P. Fitzhenry, D. B. Leinweber, M. R. Stanford and A. G. Williams, Phys. Rev. D **62**, 094509 (2000) [hep-lat/0001018].
- [16] C. J. Morningstar and M. J. Peardon, Phys. Rev. D **56**, 4043 (1997) [hep-lat/9704011].
- [17] K. Osterwalder and R. Schrader, Commun. Math. Phys. **31**, 83 (1973); **42**, 281 (1975).
- [18] G. Parisi, Nucl. Phys. B **254**, 58 (1985).
- [19] C.R. Allton *et al.* [UKQCD Collaboration], Phys. Rev. **D47**, 5128 (1993) [hep-lat/9303009].
- [20] B. Bolder *et al.*, Phys. Rev. **D63**, 074504 (2001) [hep-lat/0005018].
- [21] K. Symanzik, Nucl. Phys. **B226**, 187 (1983);
- [22] M. Alford, W. Dimm, G. P. Lepage, G. Hockney and P. B. Mackenzie, Phys. Lett. **B361**, 87 (1995) [hep-lat/9507010].
- [23] N. Cabibbo and E. Marinari, Phys. Lett. **B 119**, 387 (1982).
- [24] F. D. Bonnet, D. B. Leinweber and A. G. Williams, to appear in J. Comp. Phys. [hep-lat/0001017].
- [25] M. Luscher, Nucl. Phys. **B 180**, 317 (1981).
- [26] T. R. Klassen, Phys. Rev. D **51**, 5130 (1995); R. G. Edwards, U. M. Heller and T. R. Klassen, Nucl. Phys. B **517**, 377 (1998) [hep-lat/9711003].
- [27] F. D. Bonnet, D. B. Leinweber and A. G. Williams, "Improved Smoothing Algorithms for Lattice QCD", in progress.